0026-895X/04/6603-749–760$20.00
MOLECULAR PHARMACOLOGY
Copyright © 2004 The American Society for Pharmacology and Experimental Therapeutics
Mol Pharmacol 66:749–760, 2004

Vol. 66, No. 3
2048/1172366
Printed in U.S.A.

Glutathione Depletion in CYP2E1-Expressing Liver Cells Induces Toxicity Due to the Activation of p38 Mitogen-Activated Protein Kinase and Reduction of Nuclear Factor-κB DNA Binding Activity

Defeng Wu and Arthur Cederbaum

Department of Pharmacology and Biological Chemistry, Mount Sinai School of Medicine, New York, New York

Received April 27, 2004; accepted June 11, 2004

ABSTRACT

Depletion of glutathione (GSH) from CYP2E1-expressing cells by treatment with L-buthionine sulfoximine (BSO) causes decreased cell viability. The possible role of mitogen-activated protein kinases (MAPK) in this toxicity was evaluated. SB203580 [4-(4-fluorophenyl)-2-(4-methylsulfinylphenyl)-5-(4-pyridyl)1*H*-imidazole], an inhibitor of p38 MAPK decreased the BSO-dependent toxicity in HepG2 E47 cells, which express CYP2E1 and in hepatocytes from pyrazole-treated rats. Inhibitors of extracellular signal-regulated kinase, phosphatidylinositol 3-kinase, and c-Jun amino-terminal kinase were not protective. SB203580 did not prevent the loss of GSH nor lower the increase in reactive oxygen production; hence, protection by SB203580 was downstream of the elevated oxidative stress. Treatment with BSO caused activation of p38 MAPK whereas activation of nuclear factor-κB (NF-κB) was decreased; these effects were prevented by SB203580. We speculated that the decrease in NF-κB activation prevented production of hepatoprotective factors. One such factor could be nitric oxide (NO); indeed a NO donor decreased the BSO plus CYP2E1-dependent toxicity, whereas inhibition of inducible NO synthase (iNOS) potentiated toxicity. BSO treatment down-regulated iNOS and lowered NO levels, reactions blocked by SB203580; however, protection by SB203580 was the same in the absence or presence of an iNOS inhibitor, indicating that recovery of iNOS and NO production was not the mechanism by which SB203580 afforded protection against the BSO plus CYP2E1-dependent toxicity. Presumably other protective factors besides nitric oxide may be produced from activated NF-κB when p38 MAPK is inhibited by SB203580. These results suggest that the activation of p38 MAPK by BSO treatment in CYP2E1-expressing liver cells cause a loss in NF-κB-dependent production of hepatoprotective factors. This loss, coupled to CYP2E1-generated oxidant stress, synergize to promote cell injury.

CYP2E1 metabolizes and activates many small toxicological substrates including ethanol to more reactive and toxic products and is itself also an effective generator of reactive oxygen species (Guengerich et al., 1991; Koop, 1992). GSH levels generally are decreased in ethanol-fed animal models, especially mitochondrial GSH (Fernandez-Checa et al., 1991). GSH is an important protective antioxidant against oxidative stress and toxicity by various compounds. The GSH redox status is critical for various biological events that include transcriptional activation of specific genes, modulation of redox-regulated signal transduction, regulation of cell proliferation, apoptosis, and inflammation (Brown, 1994; Rahman and MacNee, 1999). Removal of GSH after treatment with BSO, an inhibitor of γ-glutamylcysteine ligase, produced apoptosis and necrosis in HepG2 E47 cells, which over-express CYP2E1. No toxicity was found in control C34 cells or HepG2 cells over-expressing CYP3A4 (Wu and Cederbaum, 2001). Thus, removal of GSH caused oxidative stress and loss of viability in cells expressing high levels of CYP2E1.

This work was supported by U.S. Public Health Service Grants AA 06610 and AA 03312 from The National Institute on Alcohol Abuse and Alcoholism.
Article, publication date, and citation information can be found at http://molpharm.aspetjournals.org.
doi:10.1124/mol.104.002048.

ABBREVIATIONS: GSH, glutathione; E47 cells, HepG2 cells transfected with pCI-CYP2E1 plasmid; C34 cells, HepG2 cells transfected with pCI plasmid; BSO, L-buthionine sulfoximine; DCF-DA, dichlorofluorescin diacetate; ERK, extracellular signal-regulated kinase; ELISA, enzyme-linked immunosorbent assay; γ-GCL, γ-glutamylcysteine ligase; JNK, c-Jun amino-terminal kinase; LDH, lactate dehydrogenase; MAPK, mitogen-activated protein kinase; MTT, 3-(4,5-dimethylthiazolyl)-2,5-diphenyltetrazolium bromide; L-NAME, N^{ω}-nitro-L-arginine methyl ester; NAP, *N*-acetylpenicillamine; NF-κB, nuclear factor κB; NO, nitric oxide; iNOS, inducible NO synthase; PI3 kinase, phosphatidylinositol 3-kinase; PBS, phosphate-buffered saline; ROS, reactive oxygen species; SNAP, *S*-nitroso-*N*-acetylpenicillamine; SB203580, 4-(4-fluorophenyl)-2-(4-methylsulfinylphenyl)-5-(4-pyridyl)1*H*-imidazole; PD 98059, 2′-amino-3′-methoxyflavone.

Oxidative processes may play a critical role in cellular toxicity through the activation of stress kinases such as p38 and JNK MAPK, and redox-sensitive transcription factors such as NF-κB and AP-1. These factors differentially regulate genes for proinflammatory mediators and protective antioxidants such as γ-GCL, Mn-SOD, and heme oxygenase-1 (Meyer et al., 1993; Lu, 1999). The activation of p38 MAPK can inhibit the degradation of IκB and ultimately prevent translocation of NF-κB into the nucleus and decrease NF-κB DNA binding activity (Chen et al., 2000; Granet et al., 2001). In many cells, NF-κB plays an important role in protection against cell stress that may induce apoptosis and necrosis (Mercurio and Manning, 1999; Sakon et al., 2003). We previously found that toxicity by arachidonic acid can be prevented with the p38 MAPK inhibitor SB203580 (Wu and Cederbaum, 2003).

MAPK and NF-κB activation may also affect NO synthesis (Dasilva et al., 1997). Different effects of NO on cell death and cytotoxicity have been reported depending on the experimental condition, as NO can promote apoptosis in some cells whereas it inhibits apoptosis in other cells. This complexity is a consequence of the rate of NO production and its interaction with biological molecules (Liu and Stamler, 1999). NO can inhibit cytochrome P450 activity, including that of CYP2E1 (Gong et al., 2004). The mechanism of CYP2E1-dependent oxidant stress and increase of cell toxicity is complex as the role of various signaling pathways is still unclear. In the present study, we characterized the possible role of MAPKs and PI3 kinase on toxicity found after GSH depletion in E47 cells or pyrazole-treated rat hepatocytes. We evaluated the effects of specific kinase inhibitors on the prevention of toxicity and the possible role of NF-κB or NO in this toxicity.

Materials and Methods

Rat Hepatocyte Isolation and Cell Cultures. Primary hepatocyte cultures from pyrazole-treated rats that express high levels of CYP2E1 and HepG2 cells were used as models in these experiments. Previous experiments have shown that ethanol, arachidonic acid, BSO, or iron promote greater toxicity in pyrazole hepatocytes (and E47 cells) with high levels of CYP2E1, compared with saline hepatocytes with lower levels of CYP2E1(or C34 cells with no CYP2E1) (Chen and Cederbaum, 1998; Wu and Cederbaum 2001, 2003; Gong et al., 2004). This enhanced toxicity occurs despite the increased content of GSH (and other antioxidants) which develop as an adaptive response to CYP2E1 (Mari and Cederbaum, 2000, 2001) revealing the powerful pro-oxidant actions of CYP2E1 despite enhanced antioxidant defense. Rats received humane care, and studies were carried out according to the criteria outlined in the Guide for the Care and Use of Laboratory Animals. Male Sprague-Dawley rats weighing about 150 to 170 g were injected intraperitoneally with pyrazole, 200 mg/kg body weight, once a day for 2 days to induce CYP2E1. After overnight fasting, rat hepatocytes were isolated by a two-step collagenase perfusion method (Wu et al., 1990). CYP2E1 levels were validated by Western blot analysis and catalytic activity with *p*-nitrophenol. Cell viability was evaluated by a trypan blue exclusion method and was generally around 90% for the freshly isolated hepatocytes. Hepatocytes were seeded onto 6-well plates that were coated with the basement membrane matrigel (BD Biosciences, San Jose, CA) and cultured in serum-free HeptoZyme-SFM medium (Invitrogen, Carlsbad, CA) containing 100 units/ml penicillin and 100 μg/ml streptomycin. Primary rat hepatycotes were allowed to attach to the bottom of the plate for 2 h after seeding, the medium was changed, unattached cells were gently washed out, and fresh HeptoZYME-SFM medium was added, followed by the various additions indicated below. The content of CYP2E1 declines about 50% after 1 day of culture, and about 70% after 2 or 3 days in culture in the absence of stabilizing ligand; despite this decline, as mentioned above, toxicity by ethanol, iron, arachidonic acid, or BSO is greater in the pyrazole hepatocyte than saline hepatocytes (where CYP2E1 also declines with time in culture).

E47 cells are HepG2 cells that over-express human CYP2E1, whereas C34 cells are HepG2 cells that were transfected with the pCi vector only (Chen and Cederbaum, 1998). Cells were cultured in minimal essential medium supplemented with 10% fetal bovine serum plus 100 units/ml penicillin and 100 μg/ml streptomycin in 5% CO_2 at 37°C. Before the experiment, cells were trypsinized and seeded onto 6-well plates; the amount of cells usually were between 1×10^5 to 2×10^5 or 5×10^3/well for 24-well plates. Cells were cultured in medium containing 10% serum overnight. The next day, the medium was replaced with fresh medium containing 2% fetal bovine serum. The cells were then treated with BSO and various additions.

Cellular Toxicity Determination. Pyrazole-treated rat hepatocytes or E47 cell cultures were treated with 300 μM or 1 mM BSO (Sigma-Aldrich, St. Louis, MO) in the presence or absence of 5 or 10 μM SB203580, a p38 MAPK inhibitor, 5 or 10 μM PD98059, an ERK 1/2 MAPK inhibitor, 5 or 10 μM JNK Inhibitor II (Calbiochem, San Diego, CA), a JNK MAPK inhibitor, or 5 or 10 μM wortmannin, a PI3 kinase inhibitor. The MAPK inhibitors or wortmannin were dissolved in Me_2SO and the controls were incubated with Me_2SO at a final concentration of 0.19% (v/v). Cytotoxicity was determined by either reduction of 3-(4,5-dimethylthiazol-2-yl)-2,5-diphenyltetrazolium bromide (MTT) or LDH leakage determination as described previously (Chen and Cederbaum, 1998; Gong et al., 2004). Morphological changes after treatment were also observed under the light microscope. The protection by SB203580 was further characterized by time course and dose-response experiments. To determine the effect of nitric oxide or an iNOS inhibitor on the BSO toxicity to either the pyrazole-treated rat hepatocytes or E47 cells, the nitric oxide donor SNAP (50 μM) or the iNOS inhibitor L-NAME (2 mM) was added to the cells in the presence or absence of 300 μM BSO for 72 h. LDH leakage was carried out to determine the toxicity.

Measurement of Intracellular GSH and Reactive Oxygen Production. Intracellular GSH levels were measured as described previously (Mari and Cederbaum, 2000). GSH levels were determined from a standard curve. For ROS production, pyrazole-induced rat hepatocyte cultures or E47 cells (5×10^5) were treated with 1 mM BSO or BSO plus 5 μM SB203580 for 6, 12, and 24 h. DCF-DA was added at a final concentration of 2 μg/ml, and the cells were incubated for 30 min before ending treatment. The treated cultures were washed twice with 1× PBS, trypsinized, resuspended in 3 ml of 1× PBS, and fluorescence was immediately determined in a Perkin Elmer 650–10S fluorescence spectrometer using wavelengths of 490 nm for excitation and 525 nm for emission. Background readings from cells incubated without DCF-DA were subtracted. Results are expressed as arbitrary units of fluorescence per million cells.

Activation of p38 MAPK. Pyrazole-induced rat hepatocytes or E47 cells were treated with 1 mM BSO in the absence or presence of 5 μM SB203580 for 0.5, 1.0, 2.0, 4.0, 8.0, or 12 h, respectively. The cells were harvested and sonicated in PBS for 10 s in an ice bath using a W-375 sonicator (50% duty cycle, output at 5–7 W). The cellular lysate was collected, and cell extract containing 15 μg of protein was subjected to SDS-polyacrylamide gel electrophoresis using an 8% gel. The blotted membranes were incubated with either p38 MAPK polyclonal antibody to determine the total content of p38 MAPK or monoclonal antibody against phosphorylated p38 MAPK (Santa Cruz Biotechnology, Inc., Santa Cruz, CA) to determine the content of the activated p38 MAPK (pp38). The blots were then incubated with either goat anti-rabbit or anti-mouse IgG conjugated with horseradish peroxidase for 1 h. After washing several times

with PBS containing 0.05% Tween 20, the fluorescence was developed using the enhanced chemiluminescence immune blot detection agent (ECL; Amersham Biosciences Inc., Piscataway, NJ). The arbitrary units of density of each lane were scanned with a computer software program (UN-Scan-IT, Automated Digitizing System, version 5.1; Silk Scientific Inc., Orem, UT).

NF-κB DNA Binding Activity Determination. An ELISA kit, TransAM NF-κB p65 activation assay (Active Motif Inc., Carlsbad, CA), was used to determine the NF-κB DNA binding activity. The 96-well plates were coated with an oligonucleotide that was specific for binding of p65 NF-κB in the cellular lysate. Four duplicate wells were set as controls that were either 20 pmol (2 μl) wild-type or mutated NF- κB oligonucleotide, 2.5 μg of Jurkat nuclear extract as a positive control, or the complete lysis buffer only as a blank control. Reactions were carried out per the kit manufacturer's instructions using 20 μg of cellular lysate protein. The absorbance of the yellow reaction product was determined at 450 nm with a reference wavelength of 655 nm. The results were expressed as -fold change compared with absorbance of control from day 1.

iNOS Expression and NO Content in the Medium. The expression levels of iNOS in the cells were evaluated by immnoblot analysis. E47 cells were treated with 1 mM BSO or BSO plus 5 μM SB203580 for 36 or 48 h, respectively. After treatment, cellular lysates were prepared by sonication, and the iNOS expression levels were analyzed using an iNOS monoclonal antibody (Santa Cruz Biotechnology Inc.). Nitric oxide levels in the culture medium after BSO or BSO plus various treatments were determined with the Griess reagent; briefly, E47 cells were treated as described above, 0.5 ml of culture medium from each group was collected and mixed with 0.5 ml Griess reagent (4%, w/v) at room temperature for 15 min, and the absorbance was determined at 540 nm. The content of nitric oxide was calculated according to a standard curve using sodium nitrite (Sigma-Aldrich).

Statistical Evaluation. One-way analysis of variance (analysis of variance with subsequent post hoc comparisons by Scheffe) was performed. Values reflect means ± S.E. and the numbers of experiments are given in the figure legends.

Results

P38 MAPK Inhibitor Prevents BSO Toxicity in CYP2E1-Expressing Liver Cells. Treatment with BSO was previously shown to cause a greater loss of cell viability with hepatocytes from pyrazole-treated rats with elevated levels of CYP2E1 than with saline control hepatocytes (Wu and Cederbaum, 2001). In the current study, treatment of pyrazole hepatocytes with 300 μM BSO for 72 h decreased cell viability as assayed by the MTT method (Fig. 1A). The effect of SB203580, an inhibitor of p38 MAPK, PD98059, an

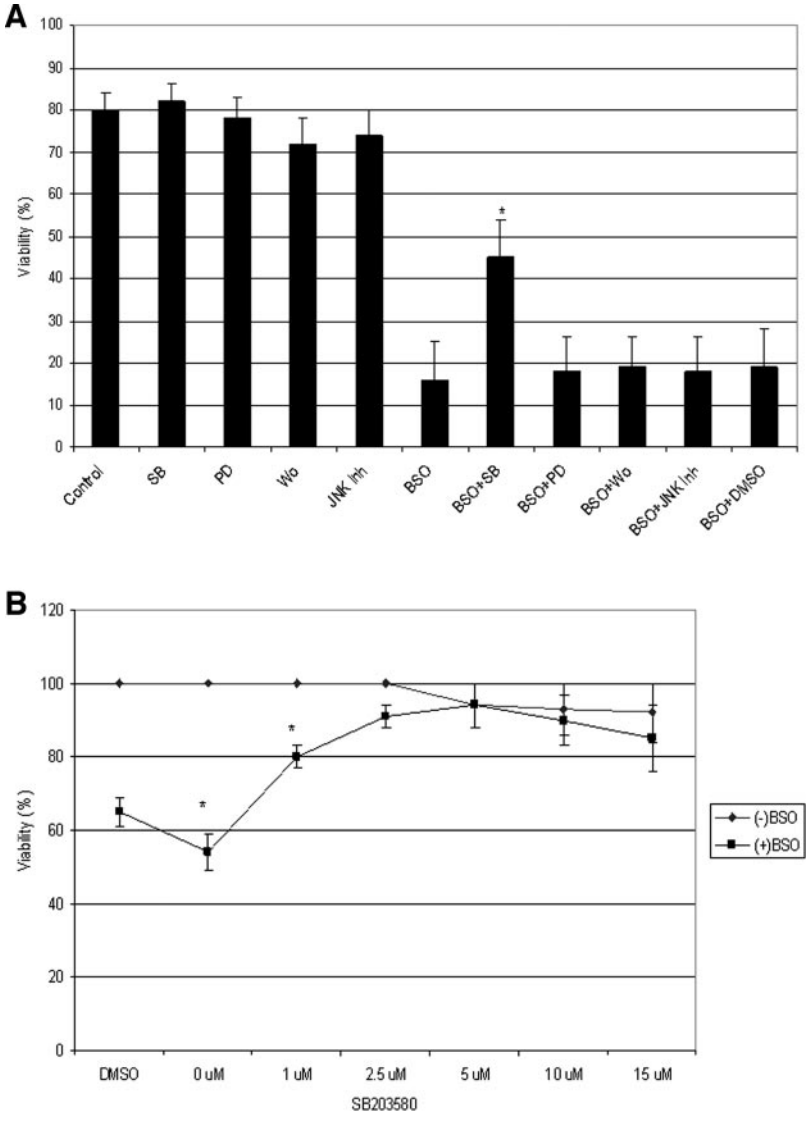

Fig. 1. p38 MAPK inhibitor SB203580 prevents BSO toxicity in pyrazole-induced rat hepatocytes. A, hepatocytes were treated with 300 μM BSO in the presence or absence of 5 μM SB203580, 5 μM PD98059, 5 μM JNK Inhibitor II, or 5 μM wortmannin for 72 h, respectively. Cell viability was determined by the MTT method. Asterisk (*) indicates significant difference compared with BSO-treated cells ($P < 0.05$). B, hepatocytes were treated with different concentrations of SB203580 in the presence or absence of 300 μM BSO for 48 h, and cell viability was determined by the MTT method. Results are from three independent experiments with duplicate samples in each group.

inhibitor of ERK 1 /2 MAPK, wortmannin, an inhibitor of PI3 kinase, or JNK inhibitor II on this toxicity was evaluated. None of these inhibitors had any effect on cellular viability in the absence of BSO. SB203580, but not the other kinase inhibitors (or the Me_2SO solvent), partially protected against the BSO-dependent toxicity (Fig. 1A). A SB203580 concentration curve was carried out after a 48-h treatment with BSO; 2.5 to 10 μM SB203580 was strongly protective against the BSO toxicity (Fig. 1B).

Similar experiments were carried out in HepG2 cells. BSO (300 μM, 72 h) produced a loss of cell viability in the E47 cells that express CYP2E1 to 46 $\pm$ 7% of control values, whereas little effect was found with the C34 cells (91 $\pm$ 8% of control values) (data not shown). SB203580 (5 μM) in the presence of BSO restored cell viability to 93 $\pm$ 8% of control values (data not shown). The other three kinase inhibitors unlike SB203580, especially PD98059 and to a lesser extent wortmannin, produced significant toxicity to the E47 (and C34) cells even in the absence of BSO (data not shown). Therefore, unlike the pyrazole hepatocytes, we could not assess the role of ERK or PI3 kinase or JNK in the BSO toxicity in the HepG2 cells in view of the toxicity of the inhibitors themselves. Nevertheless, the lack of toxicity coupled to the protection by SB203580 indicates that p38 MAPK plays a role in the BSO plus CYP2E1 toxicity. To characterize the protection by SB203580, time course and concentration-dependent experiments were carried out. BSO treatment of the E47 cells caused a time-dependent loss of cell viability over a 4-day treatment period, which was strongly prevented by 5 μM SB203580 (Fig. 2A). Near complete protection against the BSO toxicity was found with 2.5 μM SB203580 (Fig. 2B). The protection by SB203580 was also validated by assaying cell morphology changes under the light microscope (data not shown).

SB203580 Does Not Restore GSH after BSO Treatment. BSO is a specific and irreversible inhibitor of γ-glutamylcysteine ligase and BSO-induced cell toxicity is due to the depletion of intracellular glutathione levels. To evaluate whether SB203580 prevents the depletion of GSH by BSO as a possible mechanism by which it prevents cell toxicity, pyrazole-treated rat hepatocytes and E47 cells were treated with BSO or BSO plus SB203580 for 48 or 72 h, and GSH levels were determined. As shown in Fig. 3, GSH levels in the pyrazole hepatocytes decreased from control values of 54 $\pm$ 5 to 13 $\pm$ 5 and 10 $\pm$ 4 nmol/mg after 48 or 72 h of BSO treatment. In the presence of 2.5 μM or 5 μM SB203580,

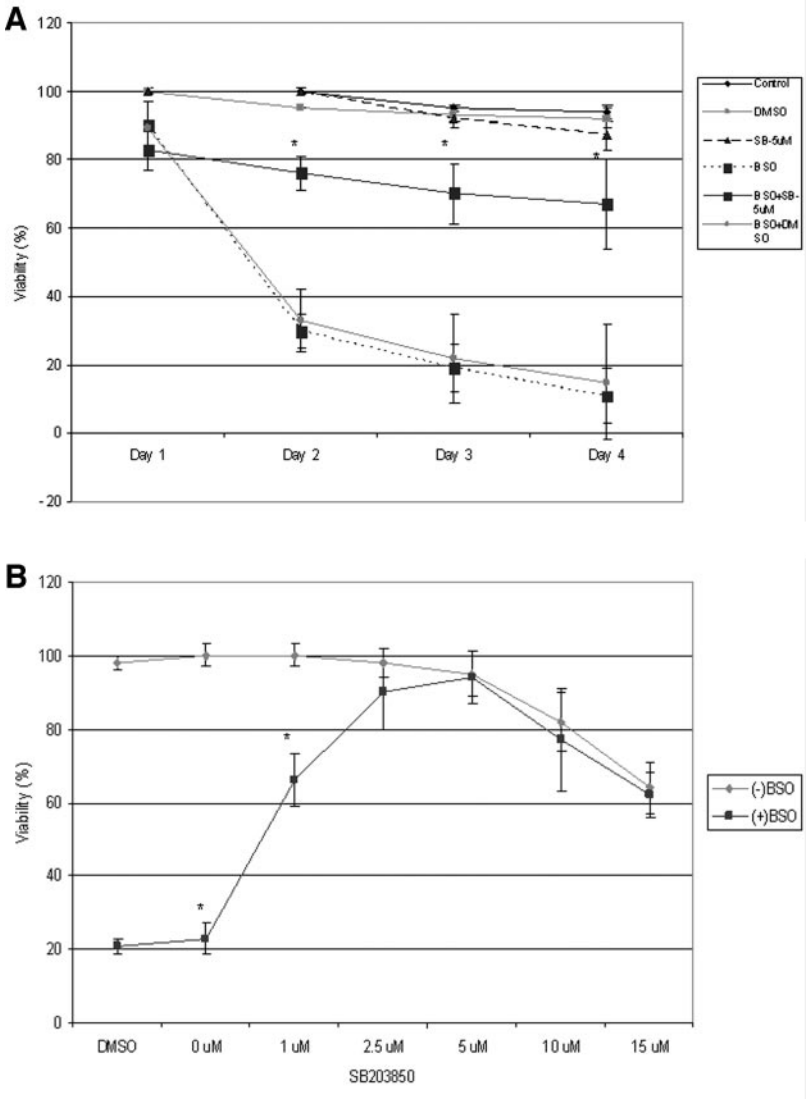

Fig. 2. SB203580 time- and concentration-dependent protection curves against BSO toxicity. A, E47 cells were treated with 5 μM SB203580 in the presence or absence of 300 μM BSO for 1, 2, 3, and 4 days, and cell viability was determined by the MTT assay. Protection by SB203580 was significant ($P < 0.05$) at day 2, 3 and 4 compared to the BSO or BSO plus Me_2SO treatments. B, E47 cells were treated with 0, 1, 2.5, 5, 10, and 15 μM SB203580 (solvent control, Me_2SO 0.19% v/v) in the presence or absence of 300 μM BSO for 72 h, and cell viability determined. Results are from three independent experiments with duplicate samples in each group.

GSH levels were not significantly restored, indicating that SB203580 does not prevent BSO toxicity by preventing the depletion of GSH by BSO. Similar results that SB203580 does not prevent the BSO-mediated depletion of GSH were found with the E47 cells (data not shown).

SB203580 Does Not Prevent the Increase in ROS Production Produced by BSO. To determine whether SB203580 prevents BSO toxicity by lowering the elevated production of ROS by the cells after BSO treatment, E47 cells or pyrazole-induced rat hepatocyte cultures were treated with 1 mM BSO in the presence or absence of 5 μM SB203580 for 6, 12, or 24 h, respectively. Because of the shorter time frame, e.g., 6 to 24 h for many of the following experiments, the BSO concentration was elevated to 1 mM to attempt to produce more "significant" effects in the shorter time span. Control experiments validated that 5 μM SB203580 provided similar protection against the toxicity of 1 mM BSO as it did against toxicity by 0.3 mM BSO, e.g., percentage of cell viability after 2 days of treatment: 0.3 mM BSO, 50%; 0.3 mM BSO + SB203580, 81%; 1 mM BSO, 35%, 1 mM BSO + SB203580, 76%. Even the strong toxicity at 72 h (35 and 19% viability with 0.3 and 1 mM BSO, respectively) was strongly prevented by SB203580 (75 and 65% viability, respectively). ROS production in the cells was determined by the DCF fluorescence method. Treatment of the pyrazole hepatocytes with BSO increased DCF fluorescence by about 2-fold after a 12- or 24-h incubation (Fig. 4). SB203580 had no effect on the basal production of ROS nor did it prevent the 2-fold increase produced by the BSO treatment (Fig. 4). Thus, the protection against loss of cell viability by SB203580 is downstream of the elevated ROS content. Similar results were observed with the E47 cells (data not shown).

BSO Activates p38 MAPK in the Liver Cells. SB203580 is a specific inhibitor of p38 MAPK. Activation of p38 MAPK may trigger signaling transduction pathways that ultimately affect cellular proliferation or viability. The prevention of BSO toxicity by SB203580 may relate to the prevention of the activation of p38 MAPK. To study whether BSO treatment leads to the activation of p38 MAPK, the pyrazole-induced rat hepatocyte cultures or E47 cells were treated with BSO or BSO plus 5 μM SB203580 for varying time points and pp38 MAPK and total p38 MAPK were determined by immunoblot analysis. In the E47 cells, p38 MAPK was not activated (0.5 to 3 h of treatment, data not shown) or after 4 h of treatment with BSO but was activated after 8 or 12 h of treatment (Fig. 5A; quantitation in Fig. 5B). p38 MAPK phosphorylation activity was induced 3- to 4-fold by BSO or BSO plus Me_2SO treatment (Fig. 5A, lanes 4 and 5 of the 8 or 12 h panels) compared with controls (lanes 1 and 2). SB203580 blocked the p38 MAPK phosphorylation induced by BSO in both the 8- and 12-h treatment groups (Fig. 5A, lane 6). p38 MAPK phosphorylation activity returned to control levels after BSO treatment for longer than 12 h (data not shown). In pyrazole-induced hepatocyte cultures, p38 MAPK phosphorylation was significantly induced 7- to 8-fold by BSO after 6 h of treatment (Fig. 5C; quantitation in Fig. 5D). SB203580 partially blocked this activation of p38 MAPK by BSO to an increase of about 4-fold compared with the control group. A 3-fold increase in pp38 MAPK was also found 12 h after BSO treatment, which was also partially prevented by SB203580. p38 MAPK phosphorylation levels returned to control values after 24 h of treatment with BSO. Thus the treatment with BSO results in activation of p38 MAPK, a reaction blocked, at least in part, by SB203580.

BSO Treatment Reduces NF-κB DNA Binding Activity. NF-κB is generally protective against the loss of cell viability, suppressing the accumulation of ROS and preventing the activation of MAPK by ROS. To study whether the BSO treatment affected the activation state of NF-κB, E47 cells were treated with 1 mM BSO or BSO plus 5 μM SB203580 for 1, 2, or 3 days, and an ELISA method was used to determine NF-κB DNA binding activity. NF-κB DNA binding activity was significantly decreased to 54 ± 3% or 38 ± 2% of the control value after 2 or 3 days of BSO treatment (Fig. 6A). SB203580 prevented the decrease of NF-κB DNA binding activity induced by BSO (Fig. 6A). Similar results were found in pyrazole-treated hepatocytes (Fig. 6B) as treatment with BSO lowered NF-κB DNA binding activity about 50% after 24 h of treatment, and SB203580 prevented this decrease.

Nitric Oxide Protects against BSO-Induced Toxicity. NO can promote toxicity in some cells under certain conditions, whereas it can inhibit toxicity in other cells/conditions. To evaluate whether NO is involved or modulates the BSO-induced toxicity, E47 or pyrazole hepatocyte cells were treated with 1 mM BSO alone or 1 mM BSO plus 50 μM of the

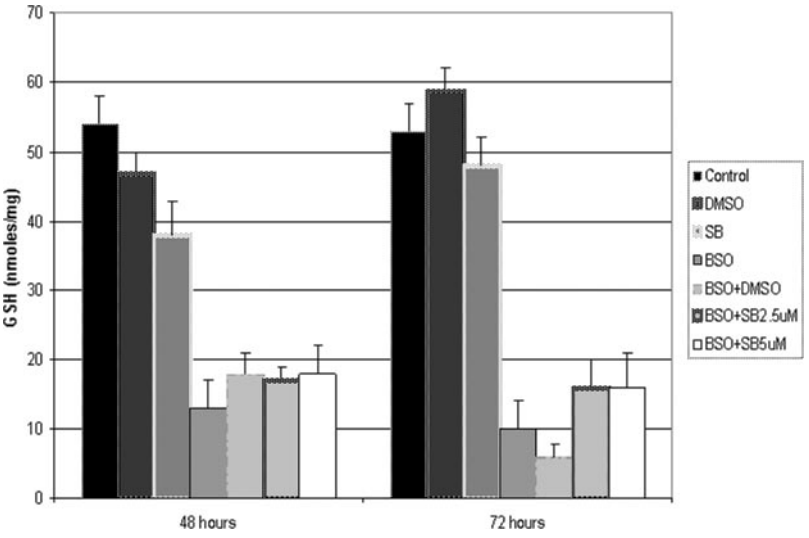

Fig. 3. SB203580 does not prevent BSO-induced GSH depletion in liver cells. Pyrazole-induced rat hepatocytes were treated with 300 μM BSO in the presence or absence of 2.5 or 5 μM SB203580 for 48 or 72 h, and cellular GSH levels were determined. No significant differences in GSH levels were observed in BSO or BSO plus Me_2SO groups compared with BSO plus SB203580 groups ($P > 0.05$). Similar results were observed in HepG2 E47 cells (data not shown). Both experiments were repeated three times and with duplicate samples in each treatment group.

NO donor SNAP or 2 mM of the iNOS inhibitor L-NAME for varying times. The effect of these treatments on BSO toxicity was evaluated by measuring LDH leakage. Treatment of the E47 cells with 1 mM BSO induced the expected cell toxicity (Fig. 7A). The NO donor SNAP reduced the BSO-induced toxicity at all time points. In contrast, L-NAME enhanced the BSO toxicity at all time points (Fig. 7A). Similar although less striking results were found with the pyrazole hepatocytes; SNAP partially protected against the BSO toxicity whereas L-NAME partially potentiated the toxicity (Fig. 7B). SNAP and L-NAME had no effects on cell viability in the absence of BSO (Fig. 7, A and B). These results suggested that NO may partially protect against the BSO toxicity, whereas reduction of intracellular NO levels may potentiate BSO toxicity. These results were validated by studying cell morphology changes: SNAP (and SB203580) prevented BSO-induced morphological changes of E47 cells, whereas L-NAME potentiated these changes (data not shown).

Effect of BSO Treatment on iNOS Content and NO Levels. Since NO can modulate the BSO-induced cytotoxicity, it was important to evaluate the effect of BSO treatment on NO production and the level of iNOS. NO levels were determined in the culture medium by the Griess reaction. SNAP increased whereas NAP and SB203580 had no effect on nitrite levels in the absence of BSO treatment (Fig. 8). After 1 mM BSO treatment for 48 h, the NO level decreased by about 40%. However, in the presence of 5 μM SB203580, the BSO-mediated lowering of NO levels was prevented. The lowest levels of NO were found in the presence of BSO plus L-NAME treatment (Fig. 8); this was the condition that produced the most powerful loss of cell viability (Fig. 7).

To correlate the decrease in NO levels by BSO treatment to effects on production of NO, levels of iNOS were determined by immunoblot analysis. Treatment with BSO for 36 or 48 h caused a decease in iNOS levels by about 50 and 80%, respectively (Fig. 9). The decline in iNOS level after a 48-h culture in the presence of BSO parallels the fall in nitrite levels after a 48-h treatment with BSO (Fig. 8). The addition of SB203580, which by itself had no effect on iNOS levels, prevented the decline produced by BSO at 48-h of treatment (Fig. 9). This prevention is associated with the elevation in nitrite levels in culture medium from cells incubated with BSO plus SB203580 compared with that in medium from cells incubated with BSO alone (Fig. 8).

Based on the above results, it appears that NO is protective against the BSO toxicity in CYP2E1-expressing liver cells. Inhibition of NO production potentiates the BSO toxicity, and continuous treatment with BSO causes a decrease in iNOS and NO production; the latter may be coupled to the increase in activation of p38 MAPK and decrease in activation of NF-κB. This led to the possibility that protection against BSO toxicity by SB203580 could be due to the prevention of the decline in iNOS and NO caused by the BSO treatment, i.e., protection by SB203580 is due to increased production of NO. If correct, L-NAME, by inhibiting iNOS should prevent the protection by SB203580. This possibility was evaluated by the experiment shown in Fig. 10. BSO treatment of the E47 cells caused an increase in LDH leakage to 63 $\pm$ 7% compared with control LDH leakage valves of less than 5%. In the presence of SB203580 or SNAP, the BSO-dependent LDH leakage declined to 30 $\pm$ 5 and 35 $\pm$ 3%, respectively, whereas with L-NAME, LDH leakage was increased to about 80 $\pm$ 6%. In the presence of SB203580 plus L-NAME, the BSO-dependent LDH leakage was largely prevented (19 $\pm$ 5%). Thus, L-NAME did not prevent the protection against BSO toxicity afforded by SB203580. Importantly, the last bar graph of Fig. 8 shows that NO levels were low in the presence of BSO plus SB203580 plus L-NAME, yet strong protection against BSO toxicity (Fig. 10, last bar graph) occurs under these conditions of low NO. These experiments were validated using the MTT assay to measure loss of cell viability (data not shown).

Discussion

The biochemical and toxicological effects of CYP2E1 have been studied in HepG2 cells engineered to express this cytochrome P450 and in cultured hepatocytes from pyrazole-treated rats with high levels of CYP2E1. The toxic effects were enhanced when cellular GSH levels were lowered by treatment with BSO. Moreover, treatment with BSO alone produced toxicity to the CYP2E1-expressing liver cells (Chen and Cederbaum, 1998; Wu and Cederbaum, 2001). GSH, therefore, appears to be critical in protecting against

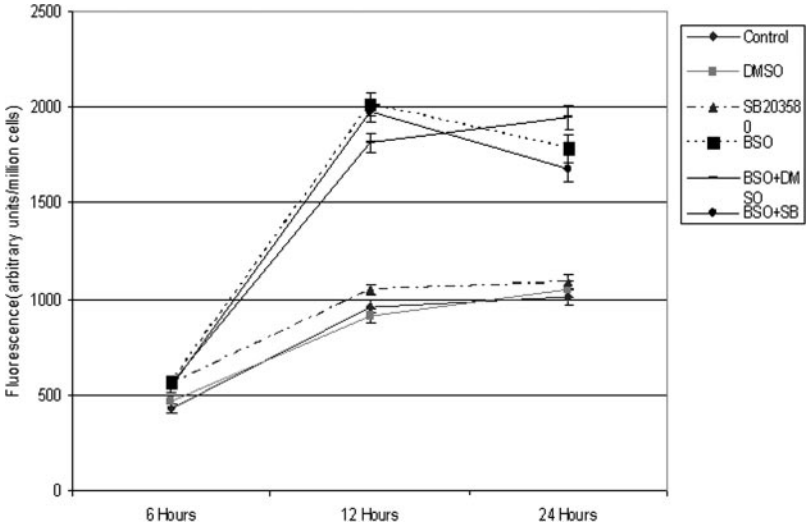

Fig. 4. SB203580 does not prevent the increase in ROS production induced by BSO. Pyrazole-induced rat hepatocytes were treated with 1 mM BSO in the presence or absence of 5 μM SB203580 for 6, 12, or 24 h, and ROS production was determined by assaying DCF fluorescence. SB203580 does not prevent the increase in ROS production induced by BSO. Similar results were observed in HepG2 E47 cells (data not shown).

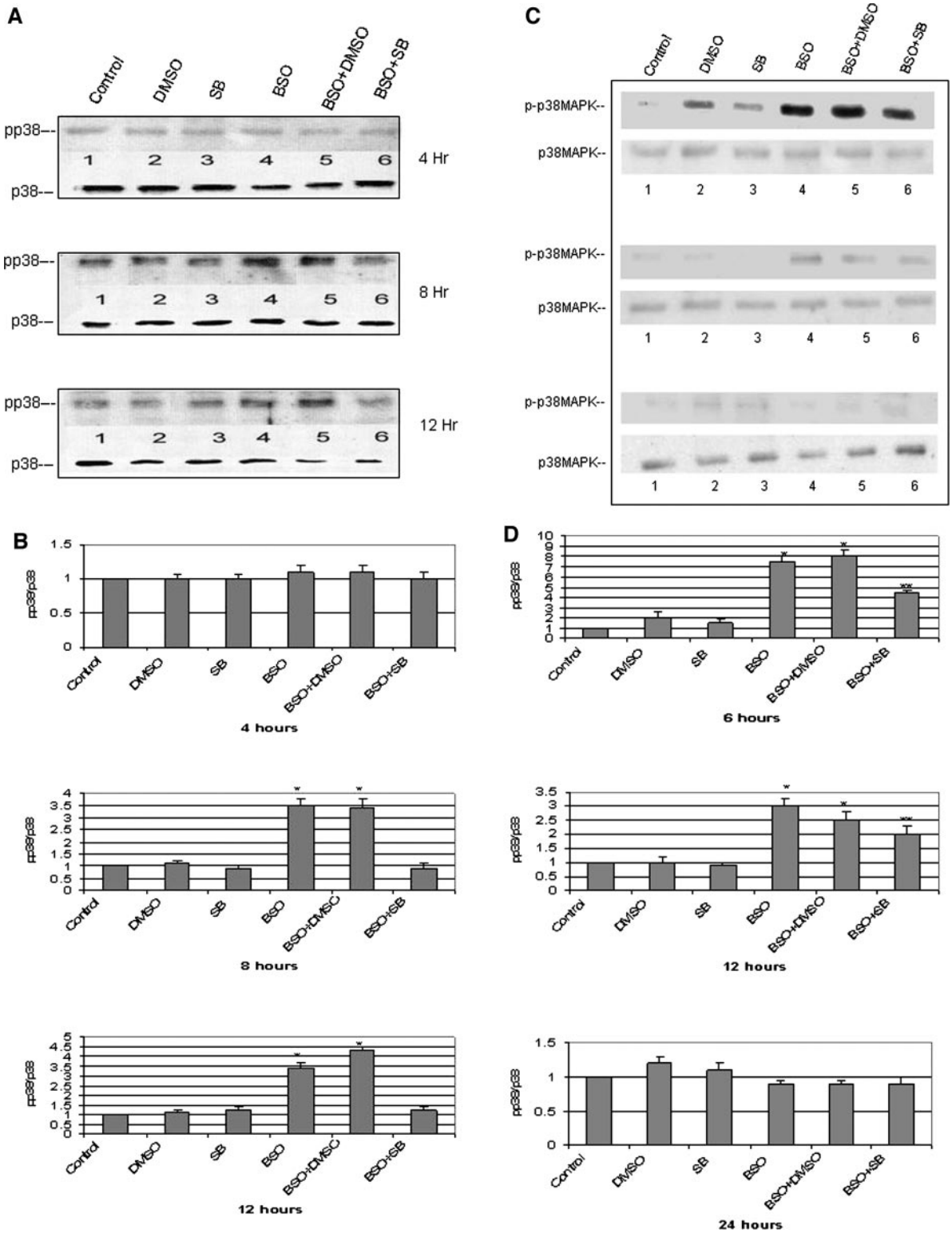

Fig. 5. BSO activates p38 MAPK in the liver cells. A, HepG2 E47 cells were treated with 1 mM BSO in the presence or absence of 5 μM SB203580 for 0.5, 1, 2 (not shown), 4, 8, or 12 h. Immunoblots were carried out to determine the content of p38 and pp38 in the cellular lysates. B, bar graphs depicting the pp38/p38 ratio. The pp38 and p38 bands were scanned and arbitrary units were determined using densitometry software. Activation of p38 MAPK was expressed by the increase in the pp38/p38 ratio. The increase of the pp38/p38 ratio was expressed as –fold increase when compared with the control ratio (1.0). Asterisks (∗) above the bars indicate a significant difference compared with the control ratio ($P < 0.05$). C, pyrazole hepatocytes were treated with 1 mM BSO in the presence or absence of 5 μM SB203580 (Me_2SO as solvent control, 0.19% v/v) for 6, 12, and 24 h. Immunoblots were carried out to determine the content of pp38 and p38 in the cellular lysates. D. The immunoblots from the hepatocytes were scanned, the arbitrary units were determined, and the pp38/p38 ratio was calculated as shown in B. Asterisks (∗) above the bars indicate a significant difference compared with the control ratio ($P < 0.05$).

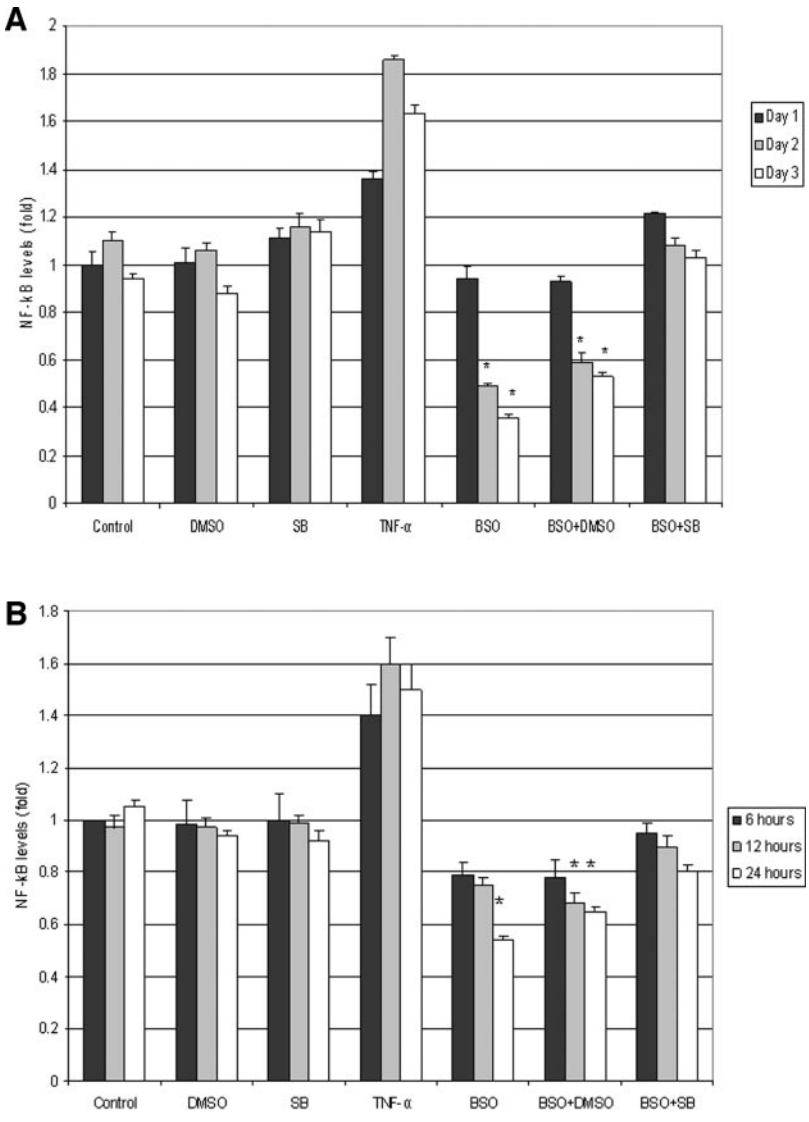

Fig. 6. BSO treatment reduces NF-κB DNA binding activity. HepG2 E47 cells or pyrazole hepatocytes were treated with 1 mM BSO in the presence or absence of 5 μM SB203580 for 1, 2, or 3 days with E47 cells or for 6, 12, and 24 h with pyrazole hepatocytes (Me_2SO or TNF-α were used as either solvent control or positive control). Cellular lysates were prepared and NF-κB DNA binding activity was determined with the TransAm NF-κB p65 activation assay kit (Active Motif Inc.). The NF-κB activity levels were expressed as -fold change compared with control. Asterisks (*) above the bars indicate a significant difference ($P < 0.05$) when compared with control. A, the results are from three independent experiments with E47 cells or with pyrazole hepatocytes (B).

CYP2E1-dependent toxicity. In fact GSH levels were higher in the E47 cells or in pyrazole-induced hepatocytes than the control cells because of an increased content and expression of γ-glutamylcysteine ligase (Mari and Cederbaum, 2000). Decreases in cellular GSH, particularly mitochondrial GSH, by chronic ethanol treatment may be a key lesion responsible for alcoholic liver injury (Fernandez-Checa et al., 1987; Colell et al., 1998).

MAPKs are involved in regulating a wide range of cellular processes and are activated in response to cellular stress and oxidant injury. ERK 1 /2, and PI3 kinase pathways are most commonly linked to regulation of cell growth and proliferation whereas the p38 and JNK MAPK pathways are more strongly tied to stress and cell toxicity. (Chang and Karin, 2001; Kyriakis and Avruch, 2001). There is also considerable overlap among these cascades both in their targets and upstream activators. We recently characterized the role of MAPKs in toxicity by arachidonic acid, a representative polyunsaturated fatty acid, in CYP2E1-dependent toxicity (Wu and Cederbaum, 2003). The goal of the current study was to evaluate the role of MAPKs in the toxicity associated with the removal of GSH from CYP2E1-expressing cells and to assess potential mechanisms for the modulation by participatory MAPKs.

ROS induce p38 MAPK phosphorylation and activation, reactions associated with decreased GSH levels and prevented by selective antioxidants including a cell permeable GSH precursor (Haddad, 2002; Haddad and Land, 2002), and p38 MAPK-mediated cytokine production and activation are inversely regulated by intracellular GSH levels (Ueda et al., 2002; Usatyuk et al., 2003). Pretreatment of alveolar epithelial cells with BSO amplified LPS activation of p38 MAPK and increased cytokine production (Haddad, 2002). SB203580 attenuated BSO-mediated facilitation of TNF-α-induced RANTES production by human bronchial epithelial cells and elevated GSH levels (Hashimoto et al., 2000, 2001). Addition of GSSG [bis(γ-glutamyl-L-cysteinylglycine) disulfide] to U937 cells caused selective induction of p38 MAPK and cell apoptosis to occur, reactions blocked by SB203580 (Filomeni et al., 2003). We evaluated possible linkage between CYP2E1, p38 MAPK, and oxidative stress in the overall pathway by which BSO treatment to remove GSH caused loss of cell viability in CYP2E1 expressing liver cells.

Depletion of GSH in the E47 cells or pyrazole hepatocytes

led to an activation of p38 MAPK. This activation occurred at relatively early time periods after the addition of BSO, e.g., 6 to 12 h, prior to developing toxicity. SB203580 offered protection against the BSO-dependent toxicity. With respect to mechanism by which SB203580 was protective against the BSO toxicity, the p38 MAPK inhibitor did not prevent the loss of GSH induced by BSO, nor did it prevent the increase in ROS generation. SB203580 had no effect on CYP2E1 levels

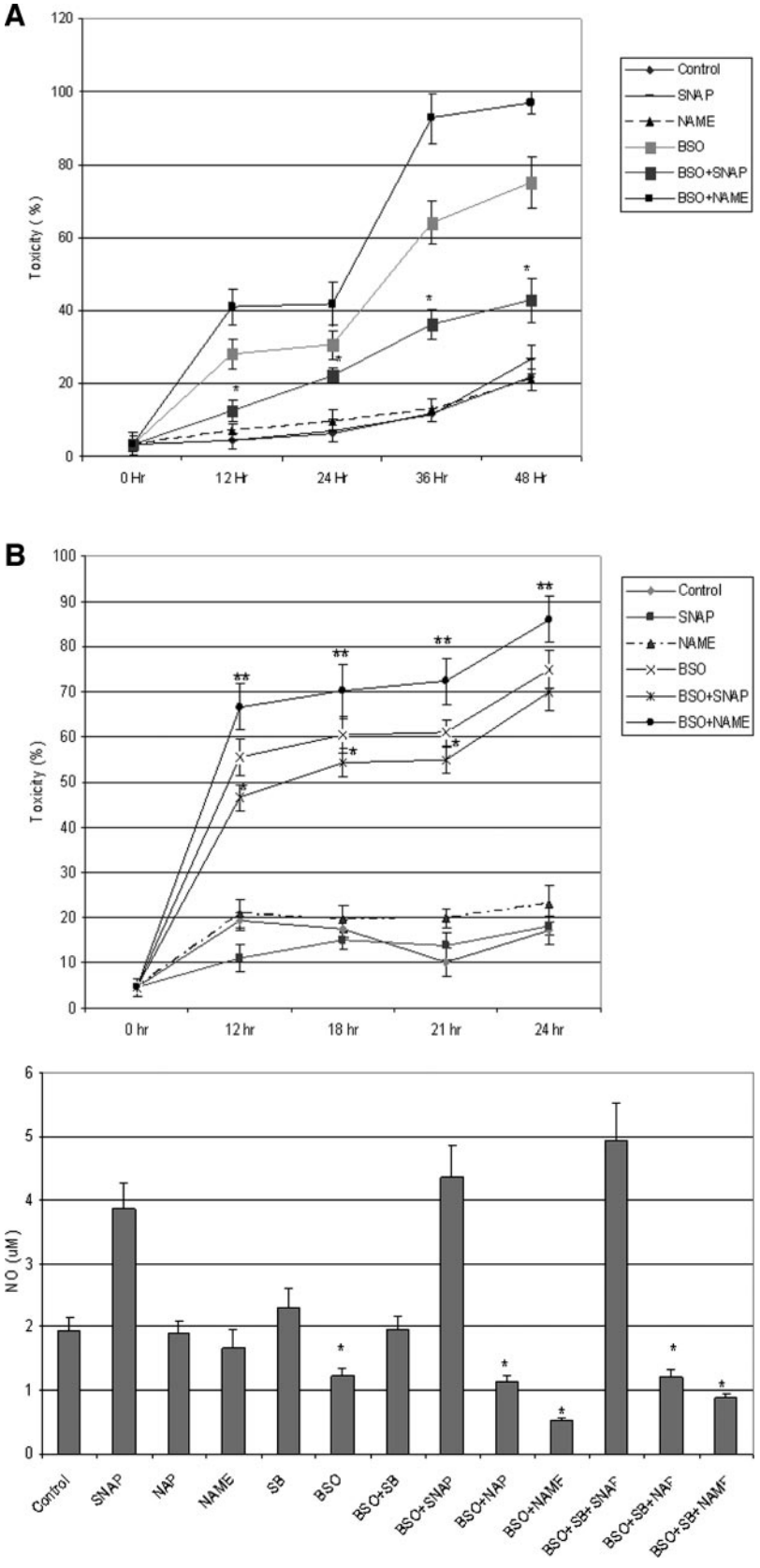

Fig. 7. Nitric oxide protects against the BSO-induced toxicity in liver cells. A, HepG2 E47 cells were treated with 1 mM BSO alone or BSO plus the NO donor SNAP (50 μM) or iNOS inhibitor L-NAME (2 mM) for 0, 12, 24, 36, and 48 h, respectively. Cell toxicity was evaluated by the LDH leakage method. B, pyrazole hepatocytes were treated with the NO donor SNAP (50 μM) or iNOS inhibitor L-NAME (2 mM) in the presence or absence of 1 mM BSO for 0, 12, 18, 21, and 24 h. Cell toxicity was evaluated by the LDH leakage method. Results are from three independent experiments with duplicate samples in each group. *, $P < 0.05$ BSO + SNAP compared with BSO alone. **, $P < 0.05$ BSO + L-NAME compared with BSO alone.

Fig. 8. BSO treatment lowers NO levels in liver cells. HepG2 E47 cells were treated with 1 mM BSO or BSO plus SNAP, L-NAME or SB203580 for 48 h. NO levels in the medium were determined by the Griess reaction method. Asterisks (*) above the bars indicate a significant difference ($P < 0.05$) when compared with control. Results were from three independent experiments with duplicate samples in each group.

or activity nor did it have significant antioxidant-like activity at the concentrations used (2.5 to 10 μM). Hence, the protection by SB203580 is downstream of the BSO plus CYP2E1-generated oxidant stress. Activation of p38 MAPK was shown to play a key role in toxicity associated with numerous insults, e.g., UV irradiation, a calcium ionophore, serum withdrawal, TNF-α, staurosporine (Kinoshita et al., 1995; Xia et al., 1995; Juo et al., 1997). Although the exact mechanisms by which activated p38 MAPK causes loss of cell viability are not clear, one intriguing target of activated p38 MAPK that we focused on was the NF-κB system. Activation of NF-κB and the subsequent production of protective/survival factors help protect hepatocytes against toxin-induced injury (Baeuerle and Henkel, 1994; Baeuerle and Baltimore, 1996). For example, hepatocytes normally are resistant to the toxic action of TNF-α mainly due to the activation of NF-κB and synthesis of survival genes (Matsumaru et al., 2003). Activated p38 MAPK can ultimately inhibit the translocation of NF-κB into the nucleus and the synthesis of survival factors (Chen et al., 2000; Granet et al., 2001). Sodium salicylate inhibits the activation of NF-κB by causing activation of p38 MAPK (Schwenger et al., 1998). We found that sodium salicylate potentiated the toxicity of BSO in the E47 cells, e.g., percentage of viability after treatment with 1 mM BSO was 85 $\pm$ 5% after 24 h and 40 $\pm$ 4% after 48 h in the absence of 10 mM sodium salicylate, and 62 $\pm$ 3% after 24 h and 16 $\pm$ 6% after 48 h of treatment with 1 mM BSO plus 10 mM sodium salicylate, respectively. Thus, an inhibitor of NF-κB potentiates BSO toxicity. Treatment with BSO caused a decrease in the basal activation of NF-κB as assessed by a DNA-NF-κB binding assay. The activation of p38 MAPK by BSO occurs earlier (6–12 h) than the decline in NF-κB binding activity by BSO (24–48 h), although exact time correlation between these two events is not clear. However, the decrease in NF-κB activation was prevented by SB203580, indicating that the decrease was mediated by activated p38 MAPK. These results suggest that loss of NF-κB activation of survival factors as a result of p38 MAPK activation may play a role in the CYP2E1 plus BSO-dependent toxicity and that the protection afforded by SB203580 may be via prevention of this loss of NF-κB activation.

Experiments were carried out to attempt to identify whether NO could be a possible NF-κB-mediated protective factor. Nitric oxide was evaluated because synthesis of NO

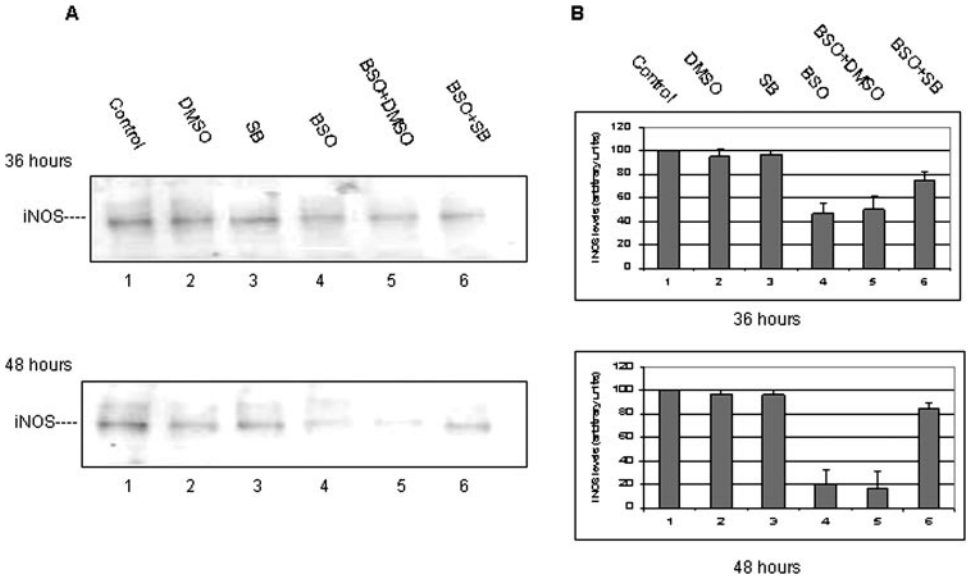

Fig. 9. BSO reduces iNOS levels in liver cells. A, HepG2 E47 cells were treated with 1 mM BSO or BSO plus 5 μM SB203580 for 36 and 48 h. Cellular lysates were prepared, and immunoblots were carried out to determine iNOS levels. Results from one experiment are shown. B, the immunoblot bands were scanned, and the arbitrary units of each band were determined with densitometry software. Results from three independent experiments (duplicate samples) are shown. Similar results were found in pyrazole hepatocytyes.

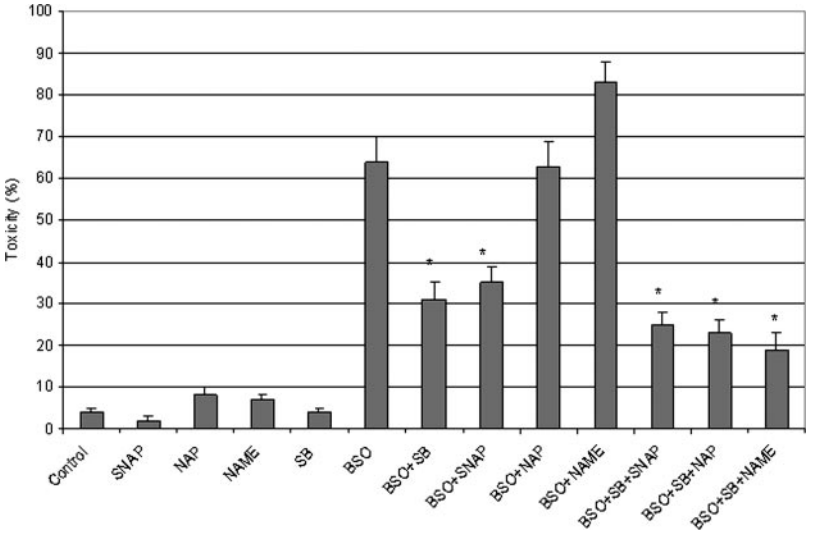

Fig. 10. L-NAME does not block SB203580 protection against BSO toxicity. HepG2 E47 cells were treated with SNAP, L-NAME, SB203580, or L-NAME plus SB203580 with or without 1 mM BSO for 48 h, and cell viability was determined by the LDH leakage method. Asterisks above the bars indicate a significant difference ($P < 0.05$) when compared with the BSO-treated group. Results are from four independent experiments.

via iNOS in hepatocytes has a general protective effect against cell injury (Gardner et al., 1998; Li et al., 1999); GSH depletion in murine hepatocytes was associated with inhibition of TNF-induced NF-κB activation of iNOS and provision of exogenous NO (SNAP) partially prevented the TNF-α plus GSH depletion toxicity (Matsumaru et al., 2003). Indeed, SNAP could partially prevent whereas L-NAME increased the CYP2E1 plus BSO-dependent toxicity, consistent with the concept that NO appears to be protective against the developing toxicity. This raised the question as to whether BSO, by activating p38 MAPK could down-regulate iNOS with reduced production of the protective NO. At 36 or 48 h after BSO treatment, iNOS levels were decreased, and this was associated with lower levels of NO (nitrite) in the culture medium. This decrease in iNOS content parallels the decrease in NF-κB activation by the BSO treatment. We speculate that the decrease in NO may contribute to a lack of or diminished hepatoprotection when GSH is depleted from the CYP2E1-expressing cells; although a loss of other NF-κB-dependent protection factors are likely to also contribute to the developing toxicity.

Could the protection by SB203580 involve restoration of iNOS and production of NO? Indeed, SB203580 elevated the low levels of iNOS and NO found after the BSO treatment to the control values. This suggests that the activation of p38 MAPK is responsible for the decline in iNOS and NO. However, to our surprise, SB203580 was as protective against the BSO-dependent toxicity in the presence of L-NAME as it was in the absence of L-NAME, suggesting that SB203580 protection was not dependent upon the production of NO. Presumably, other protective factors besides NO may be produced from activated NF-κB when p38 MAPK is inhibited by SB203580. These results do not rule out a protective role for NO because there may be NO-dependent and NO-independent hepatoprotective factors; inhibition of the NO-dependent factors may promote or increase the contributions by NO-independent factors. Future studies will be necessary to evaluate other protective factors, e.g., members of the bcl-2 family, IAP, and antioxidants such as Mn-SOD or heme oxygenase-1.

In summary, the p38 MAPK activation pathway is involved in the CYP2E1-dependent toxicity caused by GSH depletion. This toxicity can be prevented by the p38 MAPK inhibitor SB203580. The increasing activation of p38 MAPK induced by the GSH depletion with BSO inhibits NF-κB DNA binding activity and subsequent production of cell survival factors including iNOS. NO itself can lower BSO plus CYP2E1-dependent toxicity, but other hepatoprotective factors are also involved since SB203580 is still protective even in the presence of an inhibitor of iNOS and when NO levels are low. We suggest that the activation of p38 MAPK and loss of activation of NF-κB hepatoprotection produced by the depletion of GSH coupled to CYP2E1-generated ROS synergize to promote loss of cellular viability. Further studies are necessary to identify upstream and downstream mediators involved in the activation of p38 MAPK by BSO in CYP2E1-expressing cells and whether such activation occurs or plays a role in liver injury produced by chronic ethanol treatment.

References

Baeuerle PA and Baltimore D (1996) NF-kappa B: ten years after. *Cell* **87:**13–20.

Baeuerle PA and Henkel T (1994) Function and activation of NF-kappa B in the immune system. *Annu Rev Immunol* **12:**141–179.

Brown LA (1994) Glutathione protects signal transduction in type II cells under oxidant stress. *Am J Physiol* **266:**L172–L177.

Chang L and Karin M (2001) Mammalian MAP kinase signaling cascades. *Nature (Lond)* **410:**37–40.

Chen F, Ding M, Lu Y, Leonard SS, Vallyathan V, Castranova V, and Shi X (2000) Participation of MAP kinase p38 and Ikappa B kinase in chromium (VI)-induced NF-kappa B and AP-1 activation. *J Environ Pathol Toxicol Oncol* **19:**231–238.

Chen Q and Cederbaum AI (1998) Cytotoxicity and apoptosis produced by cytochrome P4502E1 in HepG2 cells. *Mol Pharmacol* **53:**638–648.

Colell A, Garcia-Ruiz C, Miranda M, Ardite E, Mari M, Morales A, Corrales F, Kaplowitz N, and Fernandez-Checa JC (1998) Selective glutathione depletion of mitochondria by ethanol sensitizes hepatocytes to tumor necrosis factor. *Gastroenterology* **115:**1541–1551.

Da Silva J, Pierrat B, Mary JL, and Lesslauer W (1997) Blockade of p38 mitogen-activated protein kinase pathway inhibits inducible nitric oxide synthase expression in mouse astrocytes. *J Biol Chem* **272:**28373–28380.

Fernandez-Checa JC, Garcia-Ruiz C, Ookhtens M, and Kaplowitz N (1991) Impaired uptake of GSH by hepatic mitochondria from chronic ethanol-fed rats. *J Clin Investig* **87:**397–405.

Fernandez-Checa JC, Ookhtens M, and Kaplowitz N (1987) Effect of chronic ethanol feeding on rat hepatocytic glutathione. Compartmentation, efflux, and response to incubation with ethanol. *J Clin Investig* **80:**57–62.

Filomeni G, Rotilio G, and Ciriolo MR (2003) Glutathione disulfide induces apoptosis in U937 cells by a redox-mediated p38 MAP kinase pathway. *FASEB J* **17:**64–66.

Gardner CR, Heck DE, Yang CS, Thomas PE, Zhang XJ, DeGeorge GL, and Laskin JD (1998) Role of nitric oxide in acetaminophen-induced hepatotoxicity in the rat. *Hepatology* **26:**748–754.

Gong P, Cederbaum AI, and Nieto N (2004) The liver-selective nitric oxide donor O2-vinyl 1-(pyrrolidin-1-yl)diazen-1-ium-1,2-diolate (V-PYRRO/NO) protects HepG2 cells against cytochrome P4502E1-dependent toxicity. *Mol Pharmacol* **65:**130–138.

Granet C, Boutahar N, Vico L, Alexandre C, and Lafage-Proust MH (2001) MAPK and SRC-kinases control EGR-1 and NF-Kappa B inductions by changes in mechanical environment in osteoblasts. *Biochem Biophys Res Commun* **284:**622–631.

Guengerich FP, Kim DH, and Iwasaki M (1991) Role of human cytochrome P-450 IIE1 in the oxidation of many low molecular weight cancer suspects. *Chem Res Toxicol* **4:**168–179.

Haddad JJ (2002) The involvement of L-gamma-glutamyl-L-cysteinyl-glycine (glutathione/GSH) in the mechanism of redox signaling mediating MAPK (p38)-dependent regulation of pro-inflammatory cytokine production. *Biochem Pharmacol* **63:**305–320.

Haddad JJ and Land SC (2002) Redox/ROS regulation of lipopolysaccharide-induced mitogen-activated protein kinase (MAPK) activation and MAPK-mediated TNF-alpha biosynthesis. *Br J Pharmacol* **135:**520–536.

Hashimoto S, Gon Y, Matsumoto K, Takeshita I, Asai Y, Asai Y, Machino T, and Horie T (2000) Regulation by intracellular glutathione of TNF-alpha-induced p38 MAP kinase activation and RANTES production by human pulmonary vascular endothelial cells. *Allergy* **55:**463–469.

Hashimoto S, Gon Y, Matsumoto K, Takeshita I, MacHino T, and Horie T (2001) Intracellular glutathione regulates tumor necrosis factor-alpha-induced p38 MAP kinase activation and RANTES production by human bronchial epithelial cells. *Clin Exp Allergy* **31:**144–151.

Juo P, Kuo CJ, Reynolds SE, Konz RF, Raingeaud J, Davis RJ, Biemann HP, and Blenis J (1997) Fas activation of the p38 mitogen-activated protein kinase signaling pathway requires ICE/CED-3 family proteases. *Mol Cell Biol* **17:**24–35.

Kinoshita T, Yokota T, Arai K, and Miyajima A (1995) Suppression of apoptotic death in hematopoietic cells by signaling through the IL-3/GM-CSF receptors. *EMBO (Eur Mol Biol Organ) J* **14:**266–275.

Koop DR (1992) Oxidative and reductive metabolism by cytochrome P450 2E1. *FASEB J* **6:**724–730.

Kyriakis JM and Avruch J (2001) Mammalian mitogen-activated protein kinase signal transduction pathways activated by stress and inflammation. *Physiol Rev* **81:**807–869.

Li J, Bombeck CA, Yang S, Kim YM, and Billiar TR (1999) Nitric oxide suppresses apoptosis via interrupting caspase activation and mitochondrial dysfunction in cultured hepatocytes. *J Biol Chem* **274:**17325–17333.

Liu L and Stamler JS (1999) NO: an inhibitor of cell death. *Cell Death Differ* **6:**937–942.

Lu SC (1999) Regulation of hepatic glutathione synthesis: current concepts and controversies. *FASEB J* **13:**1169–1183.

Mari M and Cederbaum AI (2000) CYP2E1 overexpression in HepG2 cells induces glutathione synthesis by transcriptional activation of γ-glutamylcysteine synthetase. *J Biol Chem* **275:**15563–15571.

Mari M and Cederbaum AI (2001) Induction of catalase, alpha, and microsomal glutathione S-transferase in CYP2E1 overexpressing HepG2 cells and protection against short-term oxidative stress. *Hepatology* **33:**652–661.

Matsumaru K, Ji C, and Kaplowitz N (2003) Mechanisms for sensitization to TNF-induced apoptosis by acute glutathione depletion in murine hepatocytes. *Hepatology* **37:**1425–1434.

Mercurio F and Manning AM (1999) NF-κB as a primary regulator of the stress response. *Oncogene* **18:**6163–6171.

Meyer M, Schreck R, and Baeuerle PA (1993) Hydrogen peroxide and antioxidants have opposite effects on activation of NF-κB and AP-1 in intact cells: AP-1 as secondary antioxidant-responsive factor. *EMBO (Eur Mol Biol Organ) J* **12:**2005–2015.

Rahman I and MacNee W (1999) Lung glutathione and oxidative stress implications in cigarette smoke-induced airways disease. *Am J Physiol* **277:**L1067–L1088.

Sakon S, Xue X, Takekawa M, Sasazuki T, Okazaki T, Kojima Y, Piao JH, Yagita N, Okumura K, Doi T, et al. (2003) NF-κB inhibits TNF-induced accumulation of ROS

that mediate prolonged MAPK activation and cell death. *EMBO (Eur Mol Biol Organ) J* **22:**3898–3909.
Schwenger P, Alpert D, Skolnik EY, and Vilcek J (1998) Activation of p38 mitogen-activated protein kinase by sodium salicylate leads to inhibition of tumor necrosis factor-induced IkappaB alpha phosphorylation and degradation. *Mol Cell Biol* **18:**78–84.
Ueda S, Masutani H, Nakamura H, Tanaka T, Ueno M, and Yodoi J (2002) Redox control of cell death. *Antioxid Redox Signal* **4:**405–414.
Usatyuk PV, Vepa S, Watkins T, He D, Parinandi NL, and Natarajan V (2003) Redox regulation of reactive oxygen species-induced p38 MAP kinase activation and barrier dysfunction in lung microvascular endothelial cells. *Antioxid Redox Signal* **5:**723–730.
Wu D and Cederbaum AI (2001) Removal of glutathione produces apoptosis and necrosis in HepG2 cells overexpressing CYP2E1. *Alcohol Clin Exp Res* **25:**619–628.
Wu D and Cederbaum AI (2003) Role of p38 MAPK in CYP2E1-dependent arachidonic acid toxicity. *J Biol Chem* **278:**1115–1124.
Wu DF, Clejan L, Potter B, and Cederbaum AI (1990) Rapid decrease of cytochrome P-450IIE1 in primary hepatocyte culture and its maintenance by added 4-methylpyrazole. *Hepatology* **12:**1379–1389.
Xia Z, Dickens M, Raingeaud J, Davis RJ, and Greenberg ME (1995) Opposing effects of ERK and JNK-p38 MAP kinases on apoptosis. *Science (Wash DC)* **270:**1326–1331.

Address correspondence to: Dr. Arthur I. Cederbaum, Department of Pharmacology and Biological Chemistry, Box 1603, Mount Sinai School of Medicine, One Gustave L. Levy Place, New York, NY 10029. E-mail: arthur.cederbaum@mssm.edu